



Chapter 1

Introduction

1.1 Motivation

Satellite services play an increasingly important role in our everyday life. A prominent example are Global Navigation Satellite Systems (GNSSs). The United States American Navigational Satellite Timing and Ranging Global Positioning System (NAVSTAR-GPS) program was originally launched in 1973 not only to provide means of accurate navigation but also as a reaction to the nuclear threat to the USA during the cold war [1], [2]. When the selective availability GPS feature was turned off in May 2000 ¹ its good accuracy became available for civilian use as well [3]–[6]. This caused a rapid development of everyday GNSS applications like navigation devices in cars, fleet tracking to manage transportation networks on land or sea, and measurement of absolute location and relative movement in leisure activities (hiking, geocaching, etc.). The market for GNSS applications is constantly increasing as future technologies like automated vehicles advance and the cost of GPS receiver technologies drop.

The Russian Global Navigation Satellite System GLONASS ² has been developed in parallel to GPS [7]–[11]. Currently, both are the only fully operated satel-

¹<http://www.gps.gov/systems/gps/modernization/sa/> (17.10.2015)

²<http://glonass-iac.ru/en/> (17.10.2015)

lite navigation systems with comparable precision. With increasing relevance of GNSS, additional systems are being established to avoid dependency on the GPS system and increase GNSS performance [12]–[16]. Upon its completion expected in 2020 the Chinese BeiDou Navigation Satellite System (BeiDou-2) ³ will be comprised of 35 satellites among which 30 non-geostationary satellites will provide complete coverage of the globe [17]. The European GALILEO system which is directly competitive to BeiDou-2 due to identical frequencies is currently established in space, again with an estimated completion in 2020 and 30 satellites [18]–[22]. In addition the seven-satellite Indian Regional Navigational Satellite System (IRNSS) ⁴ is to be completed in 2015 to cover the area of India and its surroundings and thus ensure signal availability independent of controlling governments of other GNSS. Moreover, satellite based augmentation systems (SBAS) improve reliability, accuracy and availability of GNSS [23]. In Europe, the European Geostationary Navigation Overlay Service (EGNOS) can reduce GNSS errors well below 10 m [15], [24]–[27]. Other SBASs are the Japanese Multi-functional Satellite Augmentation System (MSAS) and Quasi-Zenith Satellite System (QZSS), and the Indian GPS Aided Geo Augmented Navigation (GAGAN) system [28]–[30].

A direct consequence of the increasing development of GNSS is a growing demand for amplifiers at the corresponding frequencies. Summarized, all GNSS operation ranges in L-band between 1.176 and 1.617 GHz [9], [23], [31]. GPS uses frequency bands (carrier frequencies) L1 (1.57542 GHz), L2 (1.22760 GHz) and L5 (1.17645 GHz). The most important frequency for civilian use is at L1. GALILEO is currently starting operation at E5 (E5a = 1.17645 GHz and E5b=1.20714 GHz), E6 (1.27875 GHz) and E1 (1.57542 GHz) bands. It is compatible with GPS. In contrast, BeiDou-2 frequency bands (carrier frequencies) which are B1 (1.561098 GHz and 1.589742 GHz), B2 (1.20714 GHz), and B3 (1.26852 GHz) will partially overlap with both, Galileo and GPS [17].

³<http://www.beidou.gov.cn/> (17.10.2015)

⁴<http://www.isro.gov.in/irnss-programme> (17.10.2015)

GNSSs are used as an example here, but numerous other systems in L- and S-band require high-power amplifiers in space applications. Among these are IRIDIUM (L-band) and Inmarsat (S-band, among others) which provide portable satellite communication and data service usable in remote areas [32]–[41]. As the costs of GNSS receivers drop their importance augments, e.g. in extreme sports or naval applications. S-band applications are also used on other communication satellites, e.g. digital radio, weather radar, or, more prominently, for NASA’s communication with the ISS and space shuttles ⁵. Also, the “Advanced Research in Telecommunications Systems (ARTES)” program of the European Space Agency (ESA) is interested in S-band high-power amplifiers [42]. Applications are numerous. However, for the purpose of clarity this introduction continues with the GNSS example.

Invented in the 1940s traveling-wave tubes (TWTs) are an old technology [43] and have been written off in many applications when semiconductor technologies advanced [44]. By the start of the GPS development, space TWTs were the relevant technology for C-band and quickly moved on to Ku- and Ka-band. In L- and S-band and thus in GNSS, semiconductor amplifiers were used. However, the focus of GNSS application has changed significantly since its beginnings and increasingly challenging tasks arise which require better performance of GNSS amplifiers, mainly regarding radio frequency (RF) output power and signal distortion [44]–[47]. A similar development has taken place regarding other applications. As a result, development of TWTs in L- and S-band started in the 1990s, e.g. at Thales. First these tubes were intended for digital radio services and soon they became an alternative and replacement for solid-state power amplifier (SSPA)-based GNSS. Doubts about mass and size of an L-band TWT compared to an SSPA unit are cleared when looking at the full system of the RF chain including cooling efforts [44]–[46].

⁵<http://www.esa.int> > Our Activities > Telecommunications & Integrated Applications > Satellite frequency bands (17.10.2015)

In L-band or higher frequencies, TWTs outperform SSPAs in efficiency regarding power and gain. Another very important advantage of tubes is an outstanding heritage and reliability in orbit [44], [47]. More than 146 TWTs are currently in orbit with more than four million hours of operation, many of them in the GNSSs mentioned above. Additional TWTs have already been delivered and are waiting to be launched with an on-going demand for space TWTs in L- and S-band.

However, it is crucial to further improve TWTs to meet the requirements of future satellite services. An approach to improve the efficiency of TWTs by suppression of the second harmonic is introduced in this work.

1.2 Harmonic formation in TWTs

TWTs are high-power amplifiers in vacuum technology which are used in high-frequency applications. They comprise four main building blocks depicted in Fig. 1.1: The electron gun generates free electrons and focuses these into a beam of a certain radius, electron density, and current. The magnet system, usually in the form of periodic permanent magnets (PPM), focuses the electron beam inside the interaction area and thus ensures that the beam does not diverge due to space-charge forces. In the interaction area an electromagnetic wave propagates on a transmission line which is designed to ensure interaction with the electron beam. An attenuation section called sever usually divides the transmission line into two sections to ensure stability. Last but not least the spent electron beam enters the collector where as much of its remaining kinetic energy as possible is retrieved to increase the overall tube efficiency. This work focuses on the events in the interaction area, especially on the properties of the transmission line. Detailed information on all TWT components can be found, e.g., in [43].

Several delay-line structures exist as transmission lines in TWTs [43]. In this work classical helical delay lines are applied as shown in Fig. 1.1. Due to their smooth dispersion characteristics over broad frequency ranges they are still the

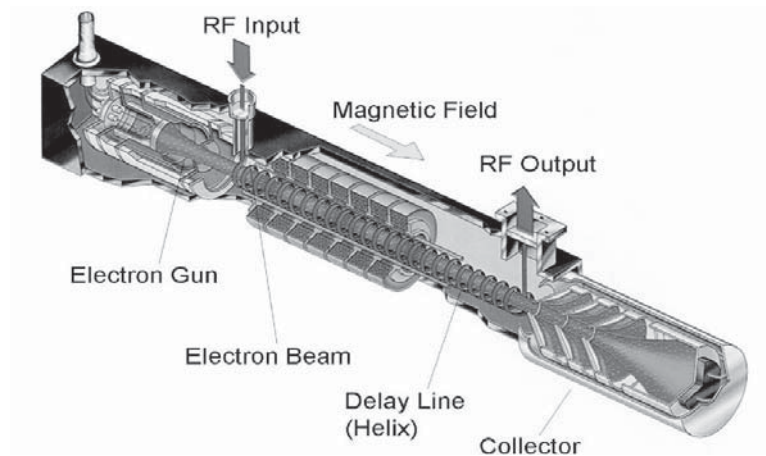
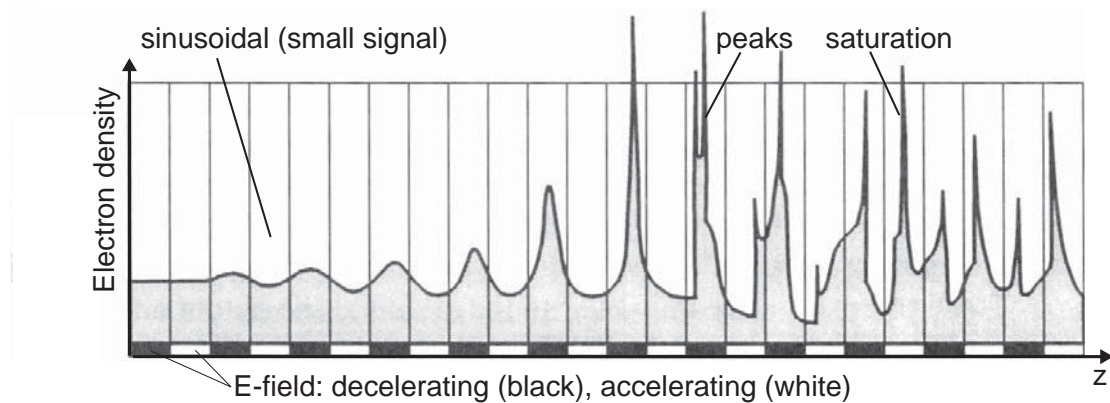


Figure 1.1: Traveling-wave tube [48].


 Figure 1.2: Development of electron bunches/charge density along the length z of a TWT [49].

most important and commonly used delay-line structure in TWTs. Beam-wave interaction occurs if the axial phase velocity of the electromagnetic (EM) wave is reduced to match the beam velocity ($v_{ph} \leq v_e$). Electrons which are located in the accelerating part of the axial electric field (E-field) get accelerated, those in the decelerating region are slowed down. In this way, electron bunches develop.

In small-signal regime the electron bunching is sinusoidal. However, closer to saturation sharply defined peaks occur which are illustrated in Fig. 1.2. As a result, the RF current on the beam does not only contain the input frequency component at first harmonic (fundamental) frequency f , but also higher harmonics, i.e.,

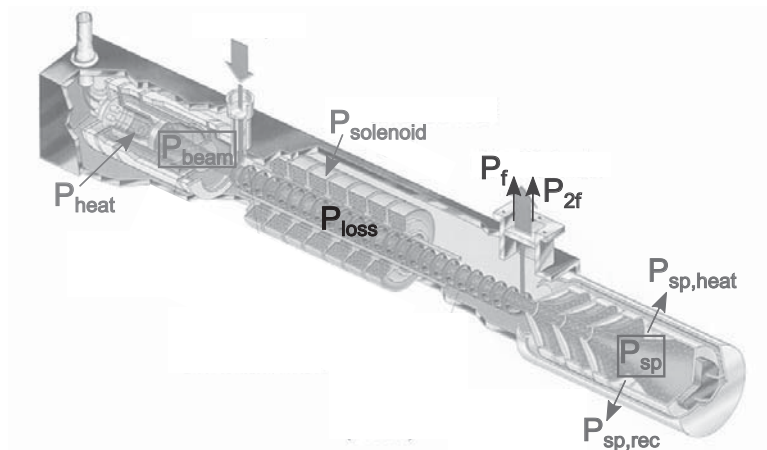


Figure 1.3: Power flow in a TWT.

waves at $2f$ (second harmonic, also referred to as “the harmonic”), $3f$, and so on.

These harmonics couple to the delay line. In this respect, the main advantage of a helical delay line becomes a disadvantage. Due to its large bandwidth, the second harmonic component is within the TWT amplification band, especially at lower frequencies of the operating band. Thus, the second harmonic is amplified and extracts energy from the electron beam.

Additionally, Fig. 1.2 illustrates saturation of the tube. The peaks in the charge density are located in regions of decelerating E-field (marked in black). As they lose kinetic energy to the EM wave amplification, the electrons are slowed down toward regions of accelerating E-field (marked in white). Here, electrons will be accelerated, taking energy from the EM wave. The process of amplification saturates.

Fig. 1.3 illustrates the power flow in a TWT. The input power is comprised of three components. P_{beam} is the electron beam power, P_{heat} is the power required to generate free electrons in the cathode, and P_{solenoid} is the power for the magnet focusing system [43]. In case of permanent magnets, power P_{solenoid} equals zero. The RF input power $P_{f,\text{in}}$ is considered negligible in comparison to P_{beam} and P_{heat} . The beam power is used to amplify the EM wave along the interaction

area. The power P_{sp} of the spent electron beam leaving the interaction area can be recovered, at least in part, by the multi-stage depressed collector ($P_{\text{sp,rec}}$). The remaining energy in the beam is lost as heat ($P_{\text{sp,heat}}$). P_{loss} describes losses in the helical transmission line. If beam power is used to amplify harmonics, it might affect the fundamental output power, as less beam energy is available for its amplification. In addition, the power is lost to the beam and thus cannot be recovered by the collector.

1.3 Specification of design goals

The main design goal of the TWTs introduced in this work is the accomplishment of the specified fundamental output power. In most tube designs presented here, this results in the requirement to increase its power level. It is to be investigated if this can be achieved by reducing the second harmonic power along the tube, resulting in the design goal of low second harmonic content.

Moreover, it will be shown that in the S-band tubes presented here, the amplitude-to-phase-modulation transfer factor (AM-to-PM transfer, k_{T}) requires monitoring during tube design [50]–[56]. It describes the change in phase of a weak carrier ω_1 due to a change in amplitude of a stronger carrier ω_2 [50]

$$k_{\text{T}} = P_{\text{in}}(\omega_2) \cdot \frac{d\Phi(\omega_1)}{dP_{\text{in}}(\omega_2)}, P_{\text{in}}(\omega_1) \ll P_{\text{in}}(\omega_2). \quad (1.1)$$

Here, the strong carrier is 20 dB above the weak one. k_{T} can be estimated using the results of single carrier tube operation [50].

Another output parameter of the tube is the power in the spent beam. Part of it can be retrieved in the collector. For high tube efficiency this part should be maximized. In the following, a new design parameter $E_{\text{e,min}}$ is introduced which serves to quantify the retrievable energy and can be used for optimization of tube performance.

Fig. 1.4 illustrates a kinetic energy spectrum of the electrons in the beam. Essentially, this plot is based on the integral over the electron energy starting from infinity. The x-axis depicts the kinetic energy of the electrons. On the y-axis the beam current which represents the amount of electrons having at least that kinetic energy is considered. This representation is useful in tube and especially collector design as the residual energy of the electrons is proportional to the (collector) voltage required to reduce their velocity to zero [43]. At the gun output (direct current (DC) beam) all electrons travel with an approximately identical velocity given by the cathode current I_0 and the accelerating voltage V_0 as illustrated by the dashed blue line. The energy spectrum at the input of the collector after beam-wave interaction is plotted in green. $E_{e,\min} = E_{e,1}$ represents the kinetic energy of the slowest electron, $E_{e,\max}$ that of the fastest. $E_{e,0}$ is the kinetic energy of an electron in the DC beam at the gun output. $E_{e,\max}$ is larger than $E_{e,0}$ because some electrons get accelerated. A multistage collector with four stages is used for this particular tube. $E_{e,1}/e$, $E_{e,2}/e$, $E_{e,3}/e$, and $E_{e,4}/e$ are the voltages V_1 , V_2 , V_3 , and V_4 of the four collector stages. The body current I_{body} or helix current I_h is caused by the electrons hitting the tube's hull or delay line. It should be small.

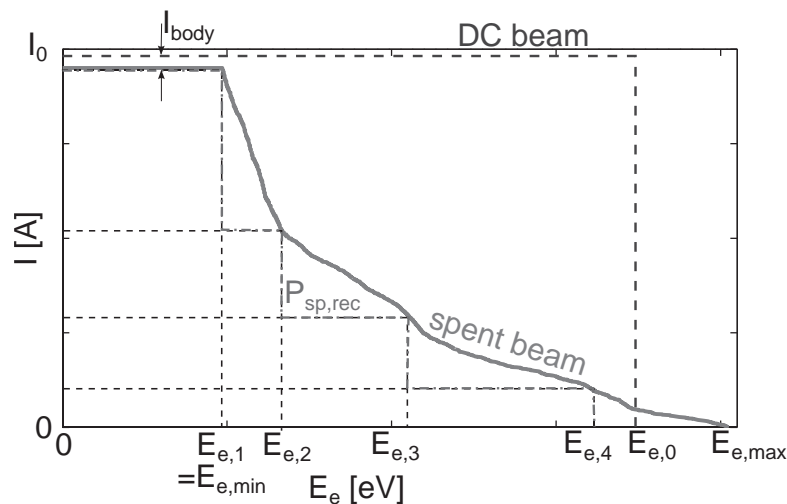


Figure 1.4: Spectrum of the kinetic energy of the electrons at the gun output (blue) and the collector input (green) and kinetic energy retrievable in the collector (red).

The area under the respective curves represents the power in the beam. The power $V_0 I_0$ of the initial DC beam (blue area) reduces to the power in the spent beam (green area) by transferring energy to the RF circuit wave at the fundamental and the harmonics. The power which can be recovered in the four-stage collector is indicated by the red area. This area needs to be maximized. It is assumed that in case of a given green curve of the energy spectrum, the collector stages are optimized to cover most of the green area. However, the first collector stage voltage $E_{e,1}/e$ must not be larger than $E_{e,\min}/e$. Otherwise, electrons might reverse direction of movement and could re-enter the interaction area where they contribute to the body current. To further increase the amount of recovered energy, it is therefore desirable to maximize the energy of the slowest electron $E_{e,\min}$. This can be achieved by reducing the harmonic content of the tube.

The maximum body current might occur below saturation (in back-off). The tube is often operated at corresponding power levels. However, the collector voltages are constant over input power. To prevent electrons from re-entering the interaction area, the minimum kinetic energy needs to be considered at various input power levels. Thus, the design parameter $E_{e,\min}$ which is used for optimization of the tube performance generally represents the minimum kinetic energy at all input power levels [57]. If $E_{e,\min}$ is considered at a specific level of input power it will be indicated.

1.4 Structure of this dissertation

As previously discussed, harmonics are a by-product of the non-linear bunching process and cannot be avoided. The TWT system needs to be insensitive to a strong second harmonic output, or else, suppression techniques are required. The aim of this work is the development of a filter for the second-harmonic component which is integrated into the delay line of the TWT. The state of technology for second-harmonic suppression prior to this work is presented in Chapter 2.1.

Moreover, the filter helix concept and a suitable simulation tool are introduced in Chapters 2.2 and 2.3, respectively. Chapter 3 deals with the implementation of the novel filter concept into TWTs. The effect of selected filters is shown in simulation and measurement results. Three different tube designs are considered, one in L- and two in S-band. The first design in L-band comprises a relatively short filter helix along an area of constant average helix pitch. It is simulated and measured in a simple helical transmission line in Chapter 3.1 and in the actual tube with electron beam in Chapter 3.2. In the second design in S-band, the number of filter cells is significantly increased which causes a filter extension into areas with a linearly decreasing average pitch (Chapter 4.1). Combinations of different filter cell lengths along one filter helix are investigated in Chapter 4.2. The third tube design introduced in Chapter 4.3 is developed with high fundamental output power tolerating high second harmonic content. The latter is reduced by filter helix application. The design aims at operation below saturation for improved linearity (Chapter 4.3.2).